**Current Biology, Volume *26***

## Supplemental Information

# The Environmental Legacy of Modern Tropical Deforestation

**Isabel M.D. Rosa, Matthew J. Smith, Oliver R. Wearn, Drew Purves, and Robert M. Ewers**

**Supplemental Information**

**Supplemental Information – Figures and Figure Legends**

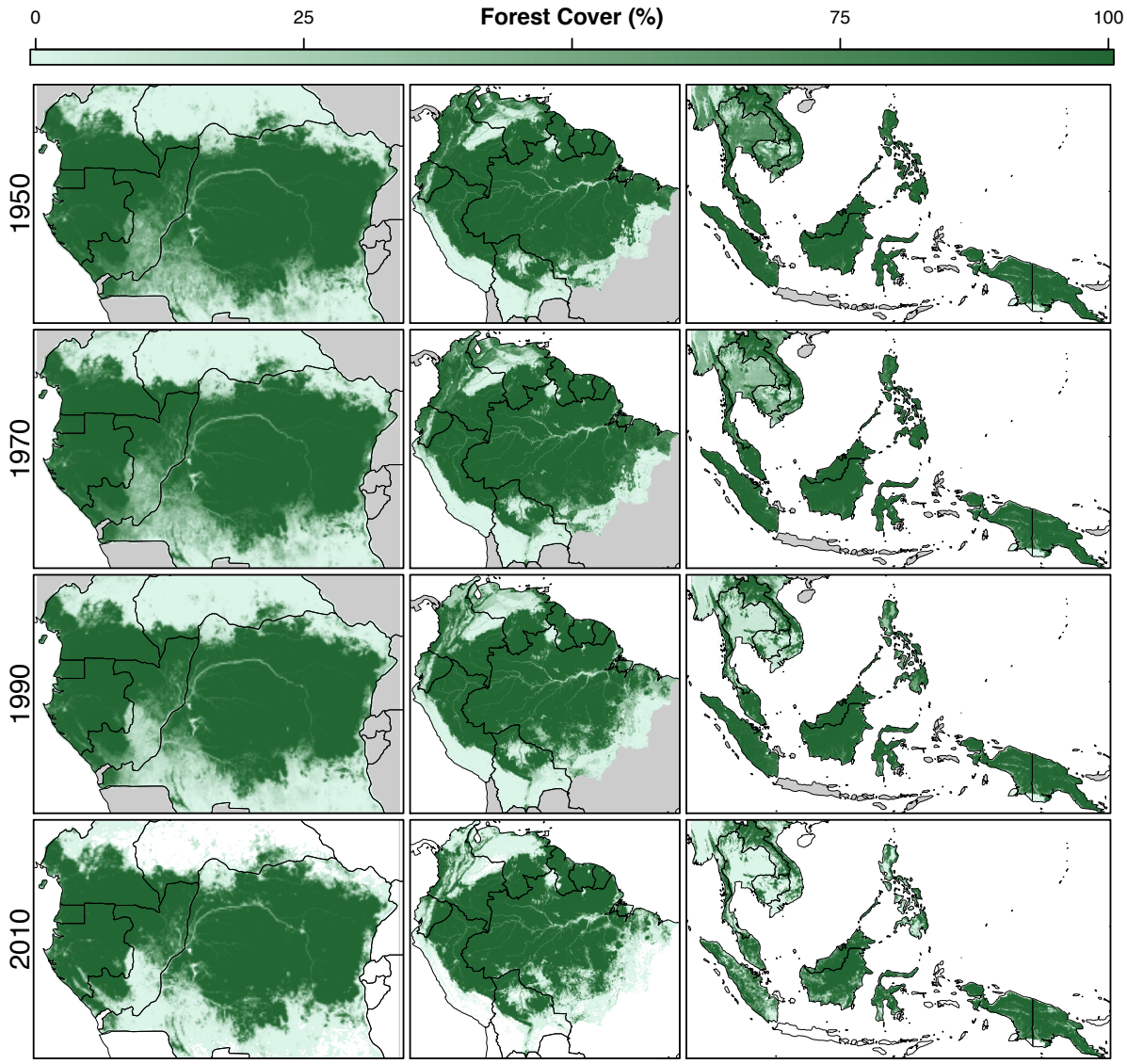


**Figure S1 –** Simulated forest cover (%) from 1950 to 2010 (observed), in 20-year time steps, at a 10 x 10 km scale. The 1950-1990 maps were produced by aggregating the 1 $km^2$ scale forest/non-forest annual maps produced by the spatially-explicit model (Related to Figure 1).

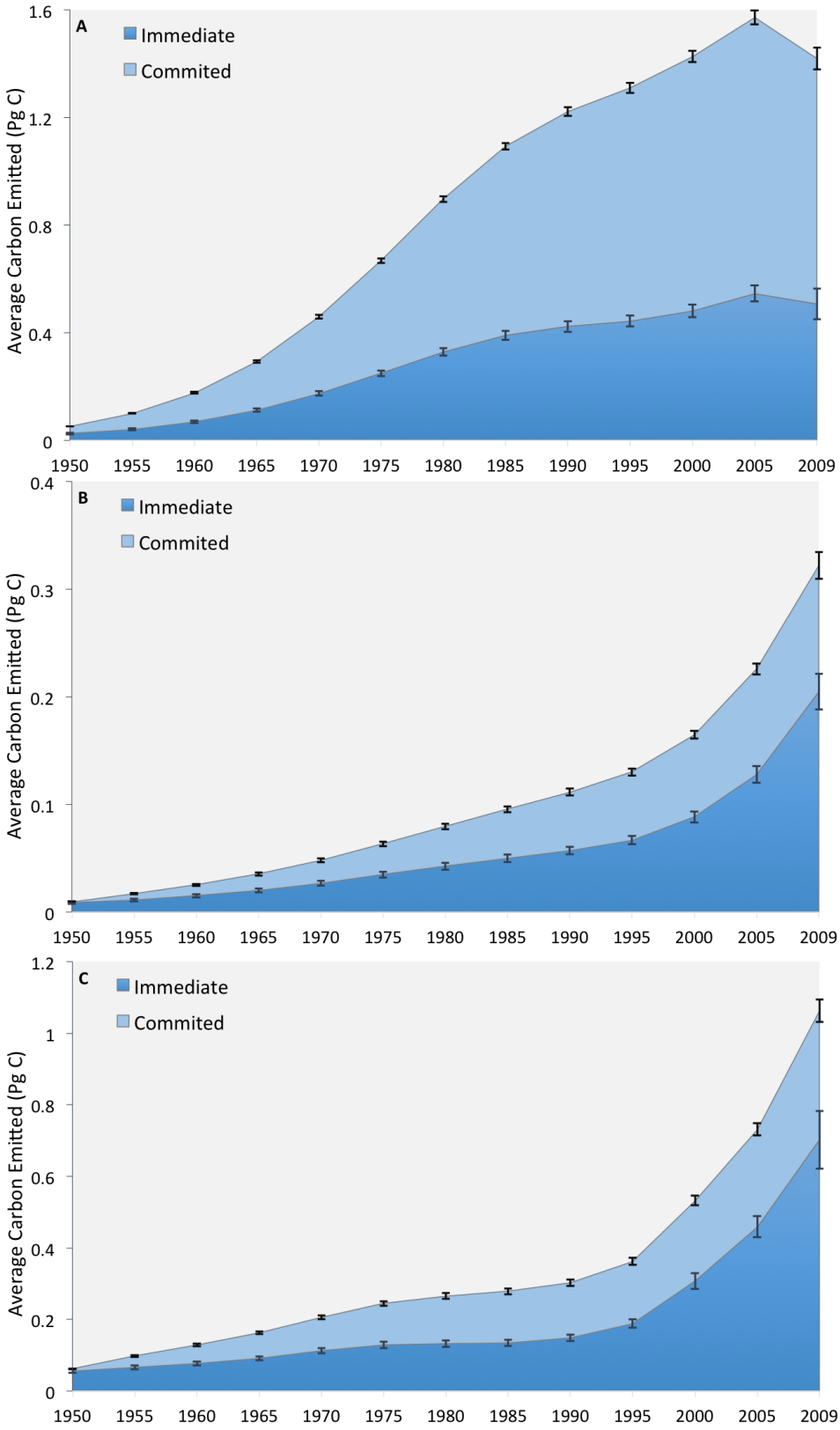


**Figure S2 –** Vegetation carbon emissions from the deforestation of tropical rainforests in (A) the Amazon, (B) the Congo basin, and (C) Southeast Asia from 1950-2009. Emissions are separated into those that occurred from deforestation that took place in that year (Immediate) and those that occurred as a result of time lags in the release of carbon from deforestation that occurred in previous years (Committed). Error bars represent the 95% confidence intervals from 100 model replicates (Related to Figure 2).

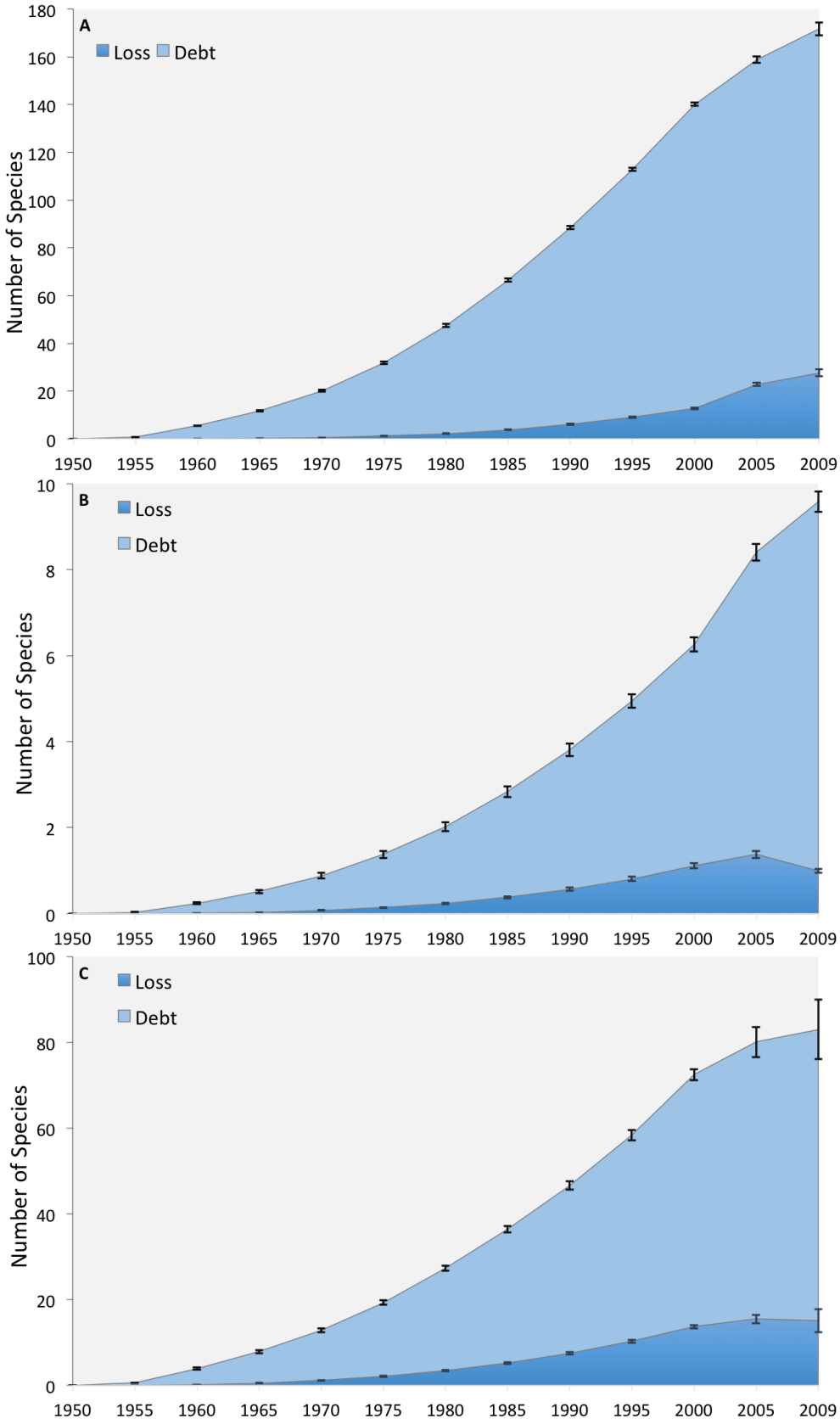


**Figure S3 –** Species losses from the deforestation of tropical rainforests in (A) the Amazon, (B) the Congo basin, and (C) Southeast Asia from 1950-2009. Species losses are separated into those that already happened (Loss) and those that will occur as a result of time delays in the extinction of species (Debt). Error bars represent the 95% confidence intervals from 100 model replicates (Related to Figure 2).

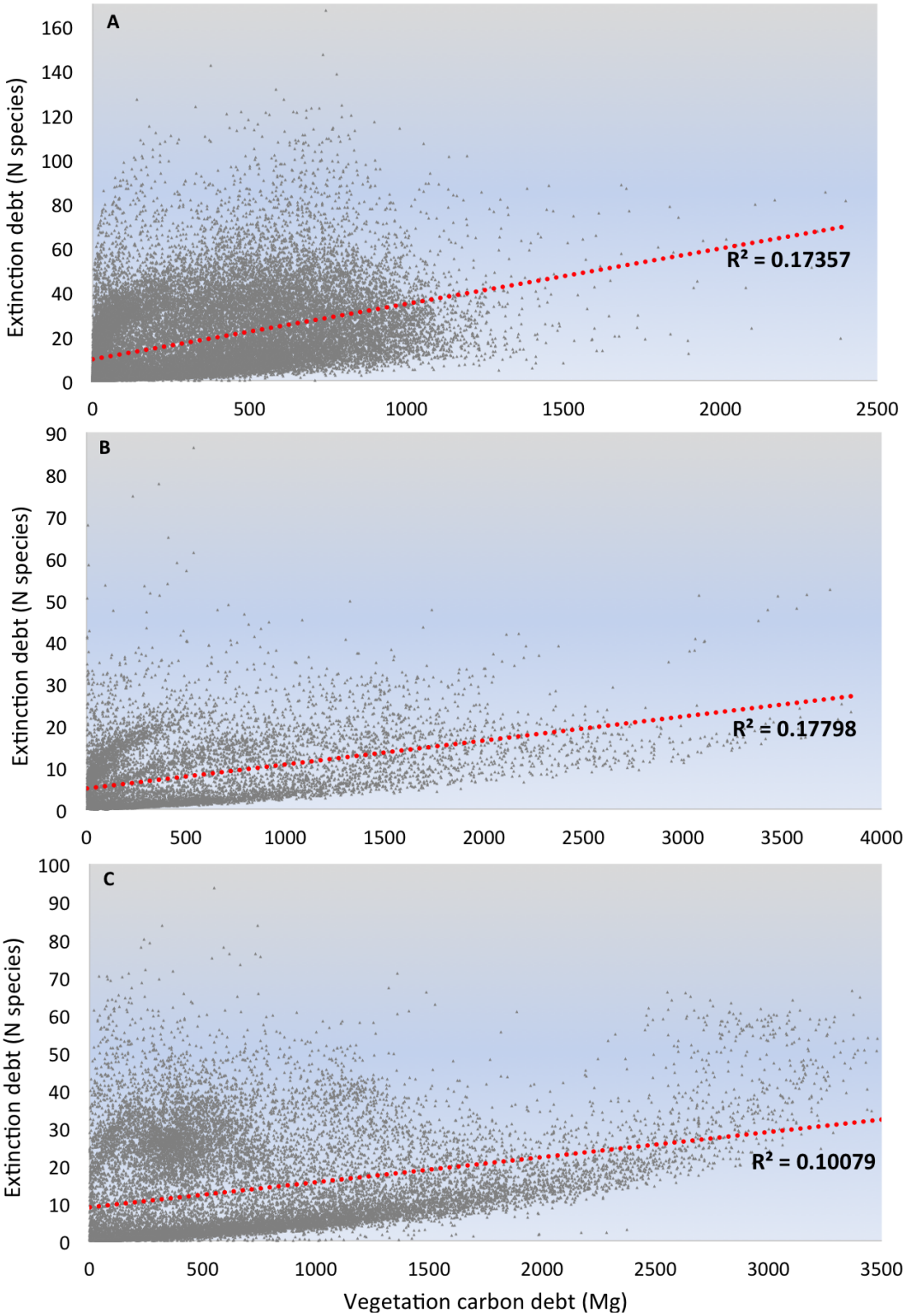


**Figure S4 –** Linear correlation (in red) between carbon and extinction debts by 2009 in (A) the Amazon, (B) the Congo basin, and (C) Southeast Asia. Each grey dot represents a 100 $km^2$ pixel. The carbon legacy was aggregated from its initial 1 $km^2$ resolution, to match the resolution of the biodiversity legacy (Related to Figure 4).

**Supplemental Information – Tables**

**Table S1 –** Historical deforestation rates in the tropics: comparison of estimates between several studies. **Related to Figure 1.**

| Reference | Time Period and Region | | | | | | | | |
|---|---|---|---|---|---|---|---|---|---|
| | Amazon | | | Congo basin | | | SE Asia | | |
| | 1980s | 1990s | 2000s | 1980s | 1990s | 2000s | 1980s | 1990s | 2000s |
| Achard et al. [S16] | – | 10,000 | – | – | 4,000 | – | – | 12,000 | – |
| | – | – | – | – | – | – | – | – | – |
| | – | 34,000 | – | – | 10,000 | – | – | 28,000 | – |
| DeFries et al. [S17] | 29,160 | 26,240 | – | 10,540 | 9,260 | – | 14,910 | 18,950 | – |
| | – | – | – | – | – | – | – | – | – |
| | 50,850 | 45,740 | – | 15,080 | 13,250 | – | 29,290 | 37,210 | – |
| FAO [S18] and Baccini et al. [S14] | – | ~40,000 | ~ 30,000 | – | – | ~6,000 | – | ~26,000 | ~12,000 |
| Harris et al. [S19, S20][1] | – | – | 41,100 | – | – | 7,360 | – | – | 14,600 |
| Hansen et al. [S15][2] | – | – | 50,101 | – | – | 12,304 | – | – | 28,184 |
| Our study - average (±s.e.) | 27,308 (±346) | 30808 (± 454) | 33,363 (±866) | 3397 (±121) | 4653 (±88) | 10,074 (±215) | 11,534 (±374) | 15,600 (±321) | 32,477 (±1561) |

*Notes:*

1 In Harris et al. [S19, S20] the deforestation rates correspond to the period between 2000 and 2005. Further, we associate their estimates for South America to our Amazon estimates, their estimates for sub-Saharan Africa to our Congo basin estimates, and their estimates for South and SE Asia to our SE Asia estimates. The geographic extents do not match perfectly, so these are approximate comparisons.

2 We calculated the average loss between 2000 and 2012, from Hansen et al. [S15] data. For each region, we used the data for the countries covered in our study. Note that Hansen's estimates include all types of forest cover, not just tropical forest.

**Table S2** – Number of unique forest-specific species estimated in each region considered in this study. **Related to Figure 3.**

| Region | Birds | Mammals | Amphibians | Total |
|---|---|---|---|---|
| Amazon | 786 | 338 | 1038 | 2162 |
| Africa | 138 | 158 | 81 | 377 |
| Mainland | 265 | 139 | 198 | 602 |
| Sumatra | 146 | 49 | 55 | 250 |
| Sulawesi | 75 | 52 | 10 | 137 |
| Borneo | 140 | 74 | 121 | 335 |
| New Guinea | 183 | 71 | 166 | 420 |
| Philippines | 171 | 62 | 55 | 288 |

**Supplemental Experimental Procedures**

Input data (and sources) to model tropical deforestation

The land cover maps used as input in our spatial model were based on the Moderate Resolution Imaging Spectroradiometer (MODIS) product called "Land Cover Type Yearly L3 Global 500 m SIN Grid V051" (full information about this product can be found here: https://lpdaac.usgs.gov/products/modis_products_table/mcd12q1), downloaded from the National Aeronautics and Space Administration (NASA) Earth Observing data and information website (http://reverb.echo.nasa.gov/reverb/). This dataset includes ten annual global land cover maps (2001-2010), each with 16 different land cover classes [S1]. Tropical rainforests, in particular, were identified by class number 2 ("Evergreen Broadleaf forest"). Additionally, we extracted the extent of agricultural lands (classes 12 and 14, respectively: "Croplands" and "Cropland/Natural vegetation mosaic") to be used as a proxy of what is already deforested. However, class 9 ("Savannas") included natural savannas as well as deforested areas. We extracted these additional deforested areas by excluding from this class areas identified as natural savanna in Worldwide Wildlife Fund (WWF) dataset on the world's biomes (http://www.worldwildlife.org/science/data/item6373.html).

We collected data on variables that could impact global land cover change from a range of sources. Global altitude and precipitation layers (30" grids) were downloaded from the WorldClim website (http://www.worldclim.org/current). The precipitation layer was used to calculate dry season length for each region based on Sombroek et al.'s [S2] methodology. Road and river maps (vector data) for each country from the Digital Chart of the World were downloaded from the DIVA-GIS website (http://www.diva-gis.org/gdata). Human population density in 2000 (30" grid) was obtained from the Gridded Population of the World website (http://sedac.ciesin.columbia.edu/gpw/), and protected areas (vector data) from the World Database of Protected Areas (http://protectedplanet.net/). The cell size used in the land cover change model was $0.01^{o}$ (~ 1 $km^2$) and the spatial projection was WGS84.

Simulating historical deforestation in the tropics

Our modelling approach is based on that of Rosa et al. [S3,S4], who developed a dynamic and spatially explicit model to predict the potential magnitude and spatial pattern of deforestation (http://stocmodlcc.net/). Usually, spatial models are used to predict the probability of future deforestation ($P_{defor\ x,t,}$ where *x* is the pixel and *t* the time step) in *t+1* within a forested area (forested pixels) given a set of variables that impact change (*e.g.* distance to roads) in *t*. Here, we inverted this and determined the probability of a deforested area in time *t* having been forested in *t-1*, the time step before ($P_{for\ x,t}$). Therefore, we constructed independent models that utilise a land cover map at time *t* with two land cover classes (forest, deforested), and for each pixel deforested at time *t*, the model calculates the probability of being forested at time *t-1*. This probability was defined as a logistic function:

$$P_{for,x,t} = 1/(1 + \exp[-\kappa_{x,t}]) \quad (1)$$

such that as $\kappa_{x,t}$ ranges from minus infinity to plus infinity, and $P_{for,x,t}$ ranges from 0 to 1.

The modelling process was initiated for each region (8 models: Amazon, Congo, and Southeast Asia was divided into Mainland Southeast Asia, Borneo, Sumatra, Papua, Sulawesi and Philippines given the contagious nature of the model) with the same set of variables: land cover and proportion of forested neighbours in the annual transition being parameterised (both dynamic variables that were updated at each time step in the model), distance to roads, distance to rivers, altitude, dry season length and population density (all static variables). Each model (for each of the nine possible annual transitions: 2002-2001 through 2010-2009) was calibrated with a forward stepwise regression to estimate the minimum adequate set of parameters required to predict change in forest cover in each time period. Specifically, for every pixel that was deforested in the year of calibration (2002-2001 through 2010-2009) we determined the probability of being forest in the year before. Each of the steps of the stepwise regression differed only in the combination of variables included in the linear models for $\kappa_{x,t}$ which were a function of the variables affecting location *x* at time *t*.

To carry out the parameter estimation it was necessary to define the log-likelihood:

$$\ell(X|s,\theta) = \sum_{x,t} log\{Z_{x,t}P_{for,x,t} + (1 - Z_{x,t})(1 - P_{for,x,t})\} \quad (2)$$

where $Z_{x,t}$ was the observed 'forest gain' at location *x* at time *t*, and *s* refers to each of the models considered during the stepwise regression, for each of the 9 annual transitions. Using the $C^{++}$ library 'Filzbach' (http://research.microsoft.com/en-us/projects/filzbach/), a posterior probability Gaussian distribution was

returned for each parameter using Markov Chain Monte Carlo sampling techniques [S3,S4]. At each step of the forward stepwise regression, a cross-validation was carried out by parameterising the model against a randomly selected subset of 50 % of locations and calculating the training likelihood, then calculating the test likelihood of the remaining 50 % of the locations, using equation 2 for validation. The 'best model' for each region, and for each annual transition (2002-2001 through 2010-2009), was selected as the one with the maximum test likelihood from all models [S3,S4].

To simulate past deforestation since 1950 until 2009, we re-applied equation 1 in each time step, recalculating the dynamic variables (*e.g.* fractional forest around each location *x*), and using a slightly different set of parameter values at each iteration (to incorporate parameter uncertainty) drawn using a Gaussian distribution from the credible interval determined above. This provided an updated $P_{for,x,t}$ for each location *x*, which was then converted to forest with that probability. In practise, this was implemented as follows: for each *x*, we drew a random number from a uniform distribution bounded at 0 and 1, and converted to forest *x* if this number was less than $P_{for,x,t}$. After these 'forest gain' events were implemented, $P_{for,x,t}$ was calculated for every location *x* again, allowing for another round of land cover change. A record of the number of cells undergoing change as well as the pattern of forest *vs.* non-forest was kept at each time step, which allowed us to calculate the annual rate of deforestation from 1950 through 2009 [S3,S4].

We accounted for three sources of uncertainty in our deforestation simulations. First, we accounted for structural uncertainty in the model by calibrating nine different models for each region using observed changes in forest cover in nine different time periods (2002-2001, 2003-2002, … , 2010-2009), which aimed to consider variability in the variables impacting deforestation over time. Instead of relying on a single time transition (*e.g.* 2002-2001) to estimate past deforestation until 1950, we took advantage of having nine annual transitions (2001 through 2010) and, for each model iteration (100 in total), we randomly selected an annual transition (2002-2001 or 2006-2005, for example), which was then used to estimate deforestation until 1950. Second, we accounted for parameter uncertainty by using the posterior distributions to randomly draw a new set of parameter values for each model iteration. Each simulation/iteration, therefore, began by randomly selecting one of the nine models to provide the posterior probability distributions for the model parameters. Then, these were sampled to obtain the specific parameter values to be used in that simulation. By running the model 100 iterations, we obtained an ensemble of 100 projections based on different initial maps of forest/deforestation and slightly different parameterised models fitted for those transitions. This allowed us to take into consideration that global land cover maps include uncertainty in their predictions of land cover change and that direct map comparisons are not recommended [S1]. Third, and finally, we allowed for model variability by employing a stochastic component, with each individual 'forest gain' event being determined randomly using a weighted probability. We ran 100 iterations of each regional deforestation model, each of which predicted the spatial pattern of forest extent backwards in time until 1950 and thereby allowed us to construct maps for each year from 1950 through 2009 representing the probability of each pixel having being deforested by that time, as well as quantifying the uncertainty surrounding our model predictions. We validated our model predictions [S3,S4] using a stringent pixel-by-pixel validation method, and accounted for near/far misses [S5] with the use of a distance-based validation metric.

Parameter estimation revealed remarkable similarities in the processes underlying the rates and patterns of historical deforestation in all three regions. Most obviously, deforestation was inferred to be highly contagious (see supplemental data set). Parameters associated with accessibility were also commonly inferred to have a significant effect on deforestation rates, especially distance to roads, in line with what is known about the process of tropical deforestation [S6-S8]. Further, the existence of protected areas, which help prevent deforestation, was often inferred to have a negative effect on deforestation rates, also in line with the land cover change modelling literature in these regions [S9-S11]. The exact parameter values associated with these processes varied substantially between regions (see supplemental data set), but there was very little variation through time within a region. This indicates that while the fundamental drivers of deforestation are similar across regions (e.g. roads are the most important proximate cause), i.e. the rank order of importance of each variable across regions is similar, their relative strengths differ, i.e. the absolute strength of the covariates varies across regions (e.g. 1 km of road in SE Asia does not have the same impact as in the Amazon).

Validation of land cover change model outputs

Model outputs were validated against observed data by calculating three metrics on a pixel-by-pixel basis: perfect match (the pixel classification in the observed and predicted maps matches exactly), omission (deforestation is observed but not predicted on that pixel) and commission (deforestation is predicted but not observed in that pixel), for the period between 2001 and 2009, both annually and cumulatively. These metrics

were chosen because, although it can be considered more rigid when compared to neighborhood metrics such as the Kappa-family [S12], it is more informative in showing how well the model predicted change [S3,S4,S13]. To avoid inflating perfect match values, by including all pixels that do not change over time in the validation process, we assessed only the predicted against the observed change. Given that different model iterations can start in different years (any year between 2002 and 2010), we did the validations based on model time (simulation time) rather than specific year. This would allow us to understand if the model was gaining or losing predictive power through simulation years, on an annual and cumulative basis. In addition, to assess if the model was able to predict the spatial pattern of change accurately and, therefore, account for near and far misses [S3,S13], we calculated a distance-based metric that allowed the quantification of the proportion of observed data that fell within a certain distance of the model predictions (1, 5, 10, 25, 50 km). In practice, we defined a buffer around each prediction and determined the number of observed change events found within that range, and then divided that number for the total change to obtain the proportion.

Model validation demonstrated that the cumulative patterns of deforestation predicted by the model were robust, although we had a relatively weak ability to simulate the exact temporal sequence of deforestation. For all models, more than 50 % of all observed deforestation events in the period 2001 through 2010 fell within 5 km of predicted deforestation, and more than two-thirds of observed deforestation fell within 10 km. Annual validations on a pixel-by-pixel basis resulted, as expected, in a weaker predictive power through time of the models in all regions. When validated against a time step further from the calibration year, the predictions became more uncertain [S4]. By contrast, when we analysed the results cumulatively, model accuracy tended to increase through time although this increase followed a non-linear pattern. This is in part explained by the fact that the number of simulations that included 9 time steps to validate gets limited (only models that were calibrated for 2010-2009 can be validated for the full 9 time steps). The best results were achieved in SE Asia, which is the region where we used sub-regional models to make the predictions. On an annual basis, omission errors tended to increase, accompanied by a decrease in the commission errors, particularly in SE Asia. As expected, the proportion of observed land cover change increased with the size of the buffer applied to our predictions and this same proportion decreased through time. This means that predictions made further from the calibration year tended to be more uncertain in concordance with pixel-by-pixel results. Through time and within 1 km (which corresponds to 1-pixel difference) of our model predictions we were able to capture from 4-9 %, 5-15 % and 4-19 % in the Amazon, Congo basin and SE Asia, respectively.

Deforestation rate comparisons

During the period from 2001 through 2010, SE Asia was the region with the highest cumulative percentage of area already deforested (32 % ± 0.31, 95 % C.I.), followed by the Amazon (18 % ± 0.55, 95 % C.I.) and finally the Congo Basin (11% ± 0.49, 95 % C.I.). Estimates of deforestation rates found in the literature are highly variable which makes it hard to properly validate them [S10], but we found our model estimates to be within the range presented by other authors (Table S1) for all three tropical regions [S14-S20], again demonstrating that our model adequately reproduces the rate and patterns of modern tropical deforestation. On average, our estimates were within the range of those found by Achard et al. [S16] for the 1990s for the Congo basin, the Amazon and SE Asia. However, if we compare with the results found by DeFries et al. [S17] our estimates are lower for the Congo basin both for the 1980s and 1990s as well as our estimates for SE Asia in the 1980s, but the estimates for the Amazon in both periods and SE Asia in the 1990s are within range. Finally, if we compare our estimates with the reports from the FAO [S18], which were also used by Baccini et al. [S14] in their study, our estimates for the Congo basin are in line for the 1990s but over the reports for the 2000s, whereas for the Amazon and SE Asia our estimates are under the estimates made by FAO in the 1990s and over the estimates for 2000s. Furthermore, comparing our results to those by Harris et al. [S19,S20], our 2000-2005 estimated average rate of deforestation for the Amazon is lower than their estimate for South America (35,490 versus 41,100 $km^2$/yr), whereas our estimate for the Congo basin is similar to their rate for sub-Saharan Africa (7,412 versus 7,360 $km^2$/yr), and our estimate for SE Asia is a lot higher than their estimate for South and Southeast Asia (28,450 versus 14,600 $km^2$/yr). Finally, our deforestation rates estimates are also in line with those by Hansen et al. [S15] with Brazil showing a slowdown in deforestation and Indonesia revealing the sharpest increase in deforestation.

Carbon emissions estimates

Most biomass maps are built using current data [S14,S21] and, as a result, areas that are currently deforested have a much lower value of carbon content than the forest they previously contained, leading to underestimates of carbon emissions. To overcome this, we used the outputs of the terrestrial carbon model

developed by Smith et al. [S22], which incorporates climate dependencies and other biophysical parameters to calculate the potential living vegetation carbon content in any area of the globe.

The potential living vegetation carbon map comes from a model based on data-constrained parameters of all component processes (*e.g.* vegetation carbon, leaf mortality, land burned, biomass allocation, and fixation rate) within the global terrestrial carbon cycle. The majority of these processes were found to have strong climate dependencies [S22]. Their terrestrial carbon model predicted global patterns of equilibrium vegetation carbon (with a measure of uncertainty), which were used in this study to determine the amount of vegetation carbon lost due to deforestation. Each iteration used a slightly different map drawn from the median and uncertainty maps provided by Smith et al. [S22]. The distribution of plant carbon in each of the three regions revealed that the Amazon had a median 165.9 C t/ha (interquantile range (IQR) = 34.8), the Congo basin had a median of 170.4 C t/ha (IQR = 21.1) and Southeast Asia had a median 160.3 C t/ha (IQR = 13.4). Unsurprisingly, the spatial distribution of the vegetation carbon used in this study was found to be much smoother (potential carbon) compared to other biomass maps [S14,S21], derived from field observations and remote sensing (actual carbon). Nonetheless, there is no systematic bias and the vegetation carbon estimates are compatible with each other.

We incorporated uncertainty in the vegetation carbon content by drawing a set of 100 pan-tropical maps of living vegetation carbon, one to be used in each model iteration. Then, carbon emissions were calculated by overlapping these vegetation carbon maps with our deforestation predictions from 1950 through 2009, on an annual basis. Following a deforestation event, carbon was emitted according to a widely used bookkeeping carbon model [S14,S23,S24], slightly modified to incorporate uncertainty. This model determines that once a pixel of forest is cleared, carbon is lost (1) immediately (20%) and (2) through time by the decay of slash left in the site (70%, at a decay rate of 0.1/yr), resultant forest products (8%, at a decay rate of 0.1/yr) and elemental carbon (2%, at a decay rate of 0.001/yr). However, we know that, depending on the fate of the land cleared the percentage of carbon lost immediately might vary substantially [S25,S26]. Unfortunately, estimates in the literature of the percentage of carbon lost immediately, and the fractions, and emissions rates of different types of decay, as proposed by Houghton et al. [S24], are difficult to obtain. As a result, we also attached an uncertainty factor to both the immediate and slash decay fractions. In particular, while Ramankutty et al. [S23] inverted these percentages to build two scenarios (20% for slash and 70% for immediate loss), we randomly sampled a value between 0.2 and 0.7 to act as the immediate factor (IF), with the fraction remaining as slash calculated as 0.7 – IF. IF varied between iterations of the model, thus simulating different fates of the land after clearance. Both the fraction of forest products (0.08) and elemental carbon (0.02) were kept constant. At each model year and iteration we kept a record of the amount of carbon lost from deforestation in that year (immediate emissions) and still remaining to be emitted by decay, both from that year and previous years.

Carbon emissions comparisons

Overall, our estimates for all three regions were much higher than those made by Baccini et al. [S14] and Harris et al. [S19,S20], primarily because these authors did not consider the legacy in carbon emissions. In part, however, our estimates might also be higher because the vegetation maps used in this study include roots, not just stems and leaves, as opposed to the maps used by Baccini et al. [S14] and Harris et al. [S19,S20]. By the end of our time period, our estimates of annual emissions of carbon were 0.32 Pg C/yr compared to 0.23 Pg C/yr and 0.11 Pg C/yr, respectively; for the Amazon our estimates were found to be near two times higher (0.91 versus 0.47 and 0.44 Pg C/yr, respectively); and for SE Asia our estimates were considerably higher (0.92 versus 0.11 and 0.26 Pg C/yr, respectively). When compared to the estimates for the 1990s found by Achard et al. [S16], our results are in line (1.07 ± 0.3 *versus* 1.28 ± 0.03 Pg C/yr, respectively). However, the higher estimate by these authors is probably due to the inclusion of soil carbon (dead biomass) and degradation emissions (logging), which we did not consider. Similarly, our estimates are within the range (0.5–1.4 Pg C/yr) of those predicted by DeFries et al. [S17] for the same time period. The same is not true, however, when we compare our results (0.90 ± 0.04 Pg C/yr) with those predicted by the same author for the 1980s (0.3–0.8 Pg C/yr), and this is again due to the absence of historical emissions from their calculations. When we compared our results with atmospheric observations or measurements of carbon for the 2000s we found large variation as well. For instance, Pan et al. [S28] gross estimates of carbon (2.9 ± 0.5 Pg C/yr between 1990 and 2007), which were not spatially explicit and covered a much larger area, were still well above our estimates. On the other hand, Peylin et al. [S29] estimated that the tropics were a source of 1.6 ± 0.9 Pg C/yr (net emissions) between 2001-2004, so despite the fact that the authors considered all carbon emissions (above and belowground) as well as carbon uptake by forest regrowth, which we have excluded, our estimates were fairly comparable 1.02 ± 0.03 Pg C/yr. Finally, only for the Amazon basin, Gatti et al. [S30] estimated by atmospheric observations a net emission of 0.48 ± 0.18 Pg C/yr, for 2009-2011, which are in line with our estimates (0.51 ± 0.04 Pg C/yr) for the final year of our time period (2009).

SE Asia legacy broken-down by sub-regions

From SE Asia there would be 1.40 Pg C (± 0.38, 95% C.I.) to be released from mainland Indochina, 0.84 Pg C (± 0.28, 95% C.I.) from the island of Sumatra, 0.60 Pg C (± 0.20, 95% C.I.) from the island of Borneo, 0.46 Pg C (± 0.08, 95% C.I.) from the Philippines archipelago, and 0.12 Pg C (± 0.02, 95% C.I.) both from the islands of Sulawesi, and New Guinea.

Species Losses and Extinction Debt

Following Wearn et al. [S31], forest-specific mammals and birds were defined as species that are classified as occurring only in natural forest. For amphibians, we selected species known to occur in forest only or in forest and inland wetland. Table S2 shows the number of unique forest-specific species found for each region considered in this study [S32]. To obtain the species richness for each pixel we overlaid all forest-specific species' ranges [S32,S33] and calculated the number of ranges within each grid cell. To obtain global species losses and debts we also guarded against double counting species that were present in more than one region. To do this, we used a region x species matrix of presence-absence, and combined it with our proportion extinction/debt for each region (an output of the algorithm used). Then, we multiplied the region x species matrix by the vector of proportional extinction, and for each species, obtained the product of all the non-zero values. Finally, we summed the species-level products to determine the total number of species expected to go extinct (a similar procedure was followed to aggregate the results of the six sub-regions of Southeast Asia).

The modeling framework developed by Wearn et al. [S31] take as input the amount of forest (absolute or relative, depending on the required predictions) present in a given focal area over time. For our analyses at the scale of a whole region, we therefore considered each region as a single unit and determined its forest cover over time by summing the number of forest pixels (i.e. those equal to 1) at each time step of simulations (2009-1950).

After obtaining the species richness and forest cover estimates, we used the modeling framework outlined by Wearn et al. [S31] to estimate species losses and extinction debt through time. This framework extends the species-area relationship (SAR) to incorporate community relaxation, and involves three main parameters ($c$, $z$ and $k$), apart from the input maps of species richness and forest cover. The value of $z$ corresponds to the slope of the log-log plot of the power-law SAR, and, in combination with a constant $c$, determines the equilibrium number of species in a given area of habitat. The value of $k$, on the other hand, is the relaxation constant and determines the relative speed at which species losses occur. We used Monte Carlo simulation to allow for uncertainty in our estimates of biodiversity loss and extinction debt. For each iteration of the model (100 in total) we drew a different value of $k$ and $z$ from the distributions presented by Wearn et al. [S31]. The overall bootstrap mean for z was 0.269 (0.224-0.315, 95% CI). For $k$, the bootstrap mean was 0.0122 (0.0076-0.0194, 95% CI). Therefore, we incorporated uncertainty in both $z$- and $k$-values into the final estimates of debt/loss.

The $z$- and $k$-value distributions we used in our study were based on an extensive, global-scale literature search [S31]. The mean of the $z$-value distribution was in line with that for forest fragment systems presented in Drakare et al.'s [S34] quantitative review. The mean of the $k$-value distribution was 0.012, which corresponds to a community relaxation half-life of 57 years. This number is derived from 100's of studies, but is similar to the oft-repeated estimate of 50 years, based on a study of birds in Kenya [S35]. In addition, $k$-values have been found to be constant across a wide variety of fragment sizes [S36]. The extinction debt framework we used extends the SAR to incorporate community relaxation and applying the SAR to estimate extinctions at such large spatial scales (i.e. the whole Amazon) can be problematic, due to spatial heterogeneity in species richness and habitat loss. We therefore also performed the analysis at the scale of local communities. We used a very fine spatial resolution, one-fifth finer than that used by Wearn et al. [S31], and divided all 8 regions (Amazon, Congo, and the 6 sub-regions of SE Asia) into grids of 10 x 10 km cells. Again, we aggregated the 1 $km^2$ binary (1 – forest, 0 – deforested) forest cover maps simulated with the deforestation model from 1950 up until 2009 to a 10 x 10 km scale, by summing the number of pixels equal to 1. As a result, forest cover within each grid cell could only range between 0 (no forest) and 100 $km^2$ (completely covered in forest). We then used these cell-specific trajectories of past forest loss, together with the number of species in each cell, and re-applied Wearn et al.'s [S31] model to estimate the impact of modern deforestation on the levels of local species loss and extinction debt in each cell. The average local extinction debt by 2009 is presented in Figure S3. Each grid-square contains the estimate of how many species are committed to extinction due to past destruction of forest habitat in the tropics.

Caveats of our study

Our study focused solely on losses due to past tropical deforestation. None of the analysis performed considered potential mitigation of the impacts, and that was done intentionally because our goal was to determine the magnitude of the environmental impact of deforestation in the tropics since 1950.

We focused on living vegetation emissions from gross deforestation and did not consider regeneration, other soil organic matter (other than roots) and/or logging. Regrowth and logging were not included in the analyses because the level of data is insufficient to perform the same type of analysis that is done for deforestation in primary forests. Soil carbon datasets are also highly uncertain, its response has different trajectories following deforestation, and these are thought to be small when compared to the losses caused by the removal of aboveground vegetation biomass.

One important caveat of our analysis was the fact that we were unable to include spatial and temporal variability in the fractions of carbon that were immediately lost, or decayed over time. Deforestation activities evolved over time from more artisanal slash-and-burn agriculture to large-scale industrial agriculture, which impact the landscape differently, i.e. small fragmented patches versus large clearings of forest. However, to the best of our knowledge, there are no datasets that we could have used to obtain the full history of the landscape we modelled, with the spatial resolution we used. Particularly, we would need to know how land has changed, through time, at a very high spatial resolution (1 $km^2$). Questions like (1) was the forest completely removed? (2) Did the land stayed as bare land for just a few or many years? (3) Was the forest replaced by a pasture, a permanent or a temporary cropland? (4) How much of the land was allowed to regenerate? and (5) At what rate?; are all largely un-knowable at global scale at present, but would have to be addressed in order to have rigorous spatially-explicit fractions of carbon lost immediately and decaying over time.

Regarding the extinction debt analysis, we used the IUCN species range maps, which are known to have a rather coarse spatial resolution, thus not representing completely accurately the distribution of the species in question. Further, inherently these maps, when updated, might also take into account deforestation, thus reducing the geographic range of forest-specific species. Nonetheless, at the time of this study, this is to our knowledge the best dataset available for species occurrence, at the spatial and temporal scales we modelled in this study. Similarly, for the carbon analysis, we also only focused on species losses and immediate impacts. We did not focus on species movements, on adaptation, on mitigation strategies or take into account that some species might be able to persist in regenerating patches.

**Supplemental Information – References**


S1. Friedl, M.A., McIver, D.K., Hodges, J.C., Zhang, X.Y., Muchoney, D., Strahler, A.H., Woodcock, C.E., Gopal, S., Schneider, A., Cooper, A. et al. (2002) Global land cover mapping from MODIS: algorithms and early results. P. Soc. Photo-Opt. Ins. *83*, 287-302.

S2. Sombroek, W. (2001) Spatial and temporal patterns of Amazon rainfall - Consequences for the planning of agricultural occupation and the protection of primary forests. Ambio *30*, 388-396.

S3. Rosa, I.M.D., Purves, D., Souza Jr., C., and Ewers, R.M. (2013) Predictive Modelling of Contagious Deforestation in the Brazilian Amazon. Plos One *8*, e77231.

S4. Rosa, I.M.D., Purves, D., Carreiras, J.M.B., and Ewers, R.M. (2015) Modelling land cover change in the Brazilian Amazon: temporal changes in drivers and calibration issues. Reg. Environ. Change *15*, 1, 123-137

S5. Pontius Jr., R.G., Shusas, E., and McEachern, M. (2004) Detecting important categorical land changes while accounting for persistence. Agri., Ecosys. & Environ. *101*, 18-23.

S6. Laporte, N.T., Stabach, J.A., Grosch, R., Lin, T.S., and Goetz, S.J. (2007) Expansion of Industrial Logging in Central Africa. Science. *316*, 1451-1451.

S7. Gaveau, D.L.A., Linkie, M., Suyadi, Levang, P., and Leader-Williams, N. (2009) Three decades of deforestation in southwest Sumatra: Effects of coffee prices, law enforcement and rural poverty. Biol. Conserv. *142*, 597-605.

S8. Brandão, A.O., and Souza Jr., C.M. (2006) Mapping unofficial roads with Landsat images: a new tool to improve the monitoring of the Brazilian Amazon rainforest. Int. J. Remote Sens. *27*, 177 - 189.

S9. Gaveau, D.L., Epting, J., Lyne, O., Linkie, M., Kumara, I., Kanninen, M., and Leader - Williams, N., (2009) Evaluating whether protected areas reduce tropical deforestation in Sumatra. J. Biogeogr. *36,* 2165-2175.

S10. Duveiller, G., Defourny, P., Desclée, B., and Mayaux, P. (2008) Deforestation in Central Africa: Estimates at regional, national and landscape levels by advanced processing of systematically-distributed Landsat extracts. P. Soc. Photo-Opt. Ins. *112*, 1969-1981.

S11. Nepstad, D., Schwartzman, S., Bamberger, B., Santilli, M., Ray, D., Schlesinger, P., Lefebvre, P., Alencar, A., Prinz, E., Fiske, G. *et al.* (2006) Inhibition of Amazon deforestation and fire by parks and indigenous lands. Conserv. Biol. *20*, 65-73.

S12. Pontius, R.G., and Millones, M. (2011) Death to Kappa: birth of quantity disagreement and allocation disagreement for accuracy assessment. Int. J. Remote Sens. *32*, 4407-4429.

S13. Rosa, I.M.D., Ahmed, S.E., and Ewers, R.M. (2014) The transparency, reliability and utility of land-use and land-cover change models. Glob. Change Biol. *20*, 1707-1722.

S14. Baccini, A.G.S.J., Goetz, S.J., Walker, W.S., Laporte, N.T., Sun, M., Sulla-Menashe, D., Hackler, J., Beck, P.S.A., Dubayah, R., Friedl, M.A. *et al.* (2012) Estimated carbon dioxide emissions from tropical deforestation improved by carbon-density maps. Nat. Climate Change *2*, 182–185.

S15. Hansen, M.C., Potapov, P.V., Moore, R., Hancher, M., Turubanova, S.A., Tyukavina, A., Thau, D., Stehman, S.V., Goetz, S.J., Loveland, T.R. and Kommareddy, A. (2013) High-Resolution Global Maps of 21st-Century Forest Cover Change. Science *342*, 850-853.

S16. Achard, F., Eva, H.D., Mayaux, P., Stibig, H.J., and Belward, A. (2004) Improved estimates of net carbon emissions from land cover change in the tropics for the 1990s. Global Biogeochem. Cy. *18*, GB2008.

S17. DeFries, R.S., Houghton, R.A., Hansen, M.C., Field, C.B., Skole, D. and Townshend, J. (2002) Carbon emissions from tropical deforestation and regrowth based on satellite observations for the 1980s and 1990s. P. Natl. Acad. Sci. USA *99*, 14256-14261.

S18. Food and Agriculture Organization of the United Nations (FAO) (2010) Global forest resources assessment 2009 - main report. (Food and Agriculture Organization of the United Nations, Rome).

S19. Harris, N.L., Brown, S., Hagen, S.C., Saatchi, S.S., Petrova, S., Salas, W., Hansen, M.C., Potapov, P.V. and Lotsch, A. (2012) Baseline Map of Carbon Emissions from Deforestation in Tropical Regions. Science *336,* 1573-1576.

S20. Harris, N.L., Brown, S., Stephen, C., Baccini, A., and Houghton, R.A. (2012) Progress toward a consensus on carbon emissions from tropical deforestation. Winrock International and Woods Hole Research Center Washington, USA.

S21. Saatchi, S.S., Harris, N.L., Brown, S., Lefsky, M., Mitchard, E.T., Salas, W., Zutta, B.R., Buermann, W., Lewis, S.L., Hagen, S. *et al.* (2011) Benchmark map of forest carbon stocks in tropical regions across three continents. P. Natl. Acad. Sci. USA *108*, 24, 9899–9904.

S22. Smith, M.J., Vanderwel, M.C., Lyutsarev, V., Emmott, S., and Purves, D. (2012) The climate dependence of the terrestrial carbon cycle; including parameter and structural uncertainties. Biogeosciences *9*, 13439- 13496.

S23. Ramankutty, N., Gibbs, H.K., Achard, F., Defries, R., Foley, J.A., and Houghton, R.A. (2007) Challenges to estimating carbon emissions from tropical deforestation. Glob. Change Biol. *13*, 51-66.

S24. Houghton, R.A., Skole, D.L., Nobre, C.A., Hackler, J.L., Lawrence, K.T., and Chomentowski, W.H. (2000) Annual fluxes of carbon from deforestation and regrowth in the Brazilian Amazon. Nature *403*, 301-304.

S25. Akagi, S.K., Yokelson, R.J., Wiedinmyer, C., Alvarado, M.J., Reid, J.S., Karl, T., Crounse, J.D. and Wennberg, P.O. (2011) Emission factors for open and domestic biomass burning for use in atmospheric models. Atmos. Chem. Phys. *11*, 4039–4072.

S26. Archibald, S., Staver, A.C., and Levin, S.A. (2012) Evolution of human-driven fire regimes in Africa. P. Natl. Acad. Sci. USA 109, *3,* 847–852.

S27. Chang, D., and Song, Y. (2010) Estimates of biomass burning emissions in tropical Asia based on satellite-derived data. Atmos. Chem. Phys. *10*, 2335–2351.

S28. Pan, Y., Birdsey, R.A., Fang, J., Houghton, R., Kauppi, P.E., Kurz, W.A., Phillips, O.L., Shvidenko, A., Lewis, S.L., Canadell, J.G. *et al.* (2011) A large and persistent carbon sink in the world's forests. Science 19**,** 333, *6045*, 988-993.

S29. Peylin, P., Law, R.M., Gurney, K.R., Chevallier, F., Jacobson, A.R., Maki, T., Niwa, Y., Patra, P.K., Peters, W., Rayner, P.J. *et al.* (2013) Global atmospheric carbon budget: results from an ensemble of atmospheric $CO_2$ inversions. Biogeosciences *10,* 6699–6720.

S30. Gatti, L.V., Gloor, M., Miller, J.B., Doughty, C.E., Malhi, Y., Domingues, L.G., Basso, L.S., Martinewski, A., Correia, C.S.C., Borges, V.F. *et al.* (2014) Drought sensitivity of Amazonian carbon balance revealed by atmospheric measurements. Nature *6*; 506 (7486),76-80.

S31. Wearn, O.R., Reuman, D.C., and Ewers, R.M. (2012) Extinction debt and windows of conservation opportunity in the Brazilian Amazon. Science *337*, 228-232.

S32. International Union for Conservation of Nature (IUCN) (2014) The IUCN Red List of Threatened Species. Version 2014.1. http://www.iucnredlist.org. Downloaded in October 2014.

S33. Ridgely, R.S., Allnutt, T.F., Brooks, T., McNicol, D.K., Mehlman, D.W., Young, B.E., and Zook, J.R. (2007) Digital Distribution Maps of the Birds of the Western Hemisphere, version 3.0 (NatureServe, Arlington, VA).

S34. Drakare, S., Lennon, J. J., and Hillebrand, H. (2006) The imprint of the geographical, evolutionary and ecological context on species-area relationships. Ecol. Lett. *9*, 215-227.

S35. Brooks, T.M., Pimm, S.L., and Oyugi, J.O. (1999) Time lag between deforestation and bird extinction in tropical forest fragments. Conserv. Biol. *13.5,* 1140-1150.

S36. Wearn, O.R., Reuman, D.C., and Ewers, R.M. (2013) Response to Comment on "Extinction debt and windows of conservation opportunity in the Brazilian Amazon". Science, *339*, 271.